Journal of Sound and Vibration (2002) **249**(4), 663–678
doi:10.1006/jsvi.2001.3861, available online at http://www.idealibrary.com on IDEAL®

STRUCTURAL RESPONSE OF LAMINATED COMPOSITE SHELLS SUBJECTED TO BLAST LOADING: COMPARISON OF EXPERIMENTAL AND THEORETICAL METHODS

H. S. TÜRKMEN

Istanbul Technical University, Aeronautics and Astronautics Faculty, Maslak, Istanbul 80626 *Turkey.*
E-mails: turkmen@spinach.mae.cornell.edu; hst4@cornell.edu

(*Received* 14 *December* 2000, *and in final form* 30 *April* 2001)

The results from a theoretical and experimental investigation of the dynamic response of cylindrically curved laminated composite shells subjected to normal blast loading are presented. The dynamic equations of motion for cylindrical laminated shells are derived using the assumptions of Love's theory of thin elastic shells. Kinematically admissible displacement functions are chosen to represent the motion of the clamped cylindrical shell and the governing equations are obtained in the time domain using the Galerkin method. The time-dependent equations of the cylindrically curved laminated shell are then solved by the Runge–Kutta–Verner method. Finite element modelling and analysis for the blast-loaded cylindrical shell are also presented. Experimental results for cylindrically curved laminated composite shells with clamped edges and subjected to blast loading are presented. The blast pressure and strain measurements are performed on the shell panels. The strain response frequencies of the clamped cylindrical shells subjected to blast load are obtained using the fast Fourier transformation technique. In addition, the effects of material properties on the dynamic behaviour are examined. The strain–time history curves show agreement between the experimental and analysis results in the longitudinal direction of the cylindrical panels. However, there is a discrepancy between the experimental and analysis results in the circumferential direction of the cylindrical panels. A good prediction is obtained for the response frequency of the cylindrical shell panels.

1. INTRODUCTION

Advanced composites are being used in many applications ranging from aircraft and submarines to pressure vessels and automotive parts. For instance, aircraft interior panels, aircraft cargo liners, aircraft brakes, ballistic components, launch systems, self-contained space modules, sports equipment, naval vessels, medical equipment, rail cars, trains, and strategic and tactical missiles are some of the distinctive fields of application mentioned in the literature [1]. In all these applications, the laminated composite panel components are subjected to different loading conditions. Air blast loading is also of significant importance. The dynamic response of structures to air blast has for many years been the subject of numerous studies. Most of them are related to dynamic response of isotropic plate structures subjected to blast load [2–5]. The cylindrically curved panel structures are widely used in the aerospace industry. Cylindrical panels are fundamental parts of aircraft and rockets which could be subjected to air blast loading. However, little work on the dynamic behaviour of blast-loaded cylindrical shells has been reported to date. Redekop and Azar

0022-460X/02/040663 + 16 $35.00/0

[6] investigated the dynamic response of steel cylindrical shell panels subjected to air blast loading. The cases of rectangular and square panels having hinged and immovable boundary conditions are considered. Results from the theoretical and numerical solutions are compared for several panel cases. The dynamic response of a steel toroidal shell panel subjected to blast loading is investigated by Redekop [7]. In his paper, a series solution is obtained corresponding to a loading which is uniformly distributed on the surface of the panel, and which has a time variation described by the Friedlander decay function. In research by Jiang and Olson [8], a non-linear dynamic analysis capability is developed for isotropic, stiffened cylindrical shell structures based on a transversely curved finite strip formulation. New finite strip and finite element models have been developed for the design analysis of stiffened plate and cylindrical shell structures by Olson [9].

Some studies are related to composite material structures subjected to blast loading. Reddy [10] conducted research for the forced motions of laminated composite plates using a finite element that accounts for the transverse shear strains, rotary inertia and large rotations. Librescu and Nosier [11], in their theoretical analysis of the symmetrically laminated rectangular composite flat panels exposed to blast loading, took into account the transverse shear deformation, transverse normal stress and higher order effects. Türkmen [12] investigated the dynamic behaviour of composite plate and shell structures subjected to blast load. In his study, the theoretical solution based on the Love theory was presented. The theoretical results were compared with the experimental and finite element results. The dynamic response of a stiffened carbon fibre composite plate was obtained experimentally and numerically by Turkmen and Mecitoğlu [13]. In their study, the numerical results, which were obtained by using ANSYS finite element software, showed a good agreement with the experimental results. Recently, the dynamic response of laminated fibreglass composite plates was obtained experimentally and theoretically by Turkmen and Mecitoğlu [14]. In their study, a new displacement function was used to represent the motion of the plate. Furthermore, the finite element analysis for the blast-loaded composite plate was presented. In their study, the predicted peak strain value and the response frequency were well correlated with the experimental results. The theoretical solutions for blast-loaded composite shells were compared with the finite element results obtained by using ANSYS finite element software in the recent study of Turkmen [15]. In his study, the effect of fibre angles on the dynamic response was investigated. The response of a fibreglass fabric-laminated cylindrical panel to the blast load was investigated by Turkmen and Mecitoğlu [16].

No studies which compare the theoretical and experimental results of the blast-loaded cylindrical laminated shell are reported in the literature. The specific area of investigation in this paper is the experimental and theoretical study of the cylindrically curved laminated composite panels exposed to a normal blast shock wave. Experiments are carried out to test the cylindrically curved laminated composite panels with a clamped edges. The air blast loading is provided by a detonation wave which is generated in a tube by the reaction of liquid propane gas (LPG) and oxygen mixtures. The mathematical model of the cylindrically curved laminated composite panels subjected to blast load is developed by using the virtual work principle in the frame of Love's theory of thin elastic shells. The Runge–Kutta–Verner method is used to obtain the solution. In addition, ANSYS finite element software is utilized to obtain the strain–time history numerically. Analysis results are compared with experimental results and agreement is found. The fast Fourier transformation technique is applied on the experimental and theoretical results to obtain the response frequencies and a good prediction is obtained for the response frequency of the cylindrical shell panels. The effects of material properties on dynamic behaviour are examined.

2. EXPERIMENTAL WORK

In this study, a detonation is generated by the reaction of LPG–oxygen mixture in a circular cylindrical tube to provide the air blast loading. The detonation tube, laminated composite panel and panel mounting frame used in the tests are shown in Figure 1. The panel mounting frame is placed in front of the detonation tube. The target panel is clamped between the two steel frames with 12 bolts to satisfy the clamped boundary conditions. Thus, there are no displacements in the in-plane and out-of-plane directions on the boundaries in the tests.

The materials of panels used in the tests are the fibreglass and carbon fibre fabric composites. The test specimens are made by hand lay-up technique. Glass (181 style) or carbon fibres are laid on to a mould by hand and the AW106 resin is brushed on. The deposited layers are densified with rollers. Curing time is 3 days at the room temperature. The vacuum, which is used in this process, is 736 mm Hg. The plain weave and harness satin weave are used in the fibreglass and carbon fibre fabric composites respectively. The weight ratios of the glass fabric and the resin to the composite are equal.

Two types of panels are used in the tests. One of them, labelled "specimen I", is a five-layered fibreglass fabric (90/0° fibre orientation angle for one layer) with a thickness of 1·4 mm. The second panel labelled "specimen II" is a three-layered carbon fibre fabric (90/0° fibre orientation angle for one layer) with a thickness of 1·2 mm. The radii of curvature of the panels are 25 cm. The layers of each panel are taken to be of equal thickness. These specimens are supplied by the Turkish Airlines Maintenance Centre.

The LPG and oxygen mixture are ignited in the detonation tube to obtain the air blast pressure load which impinges against the panel. The air blast pressure distribution is

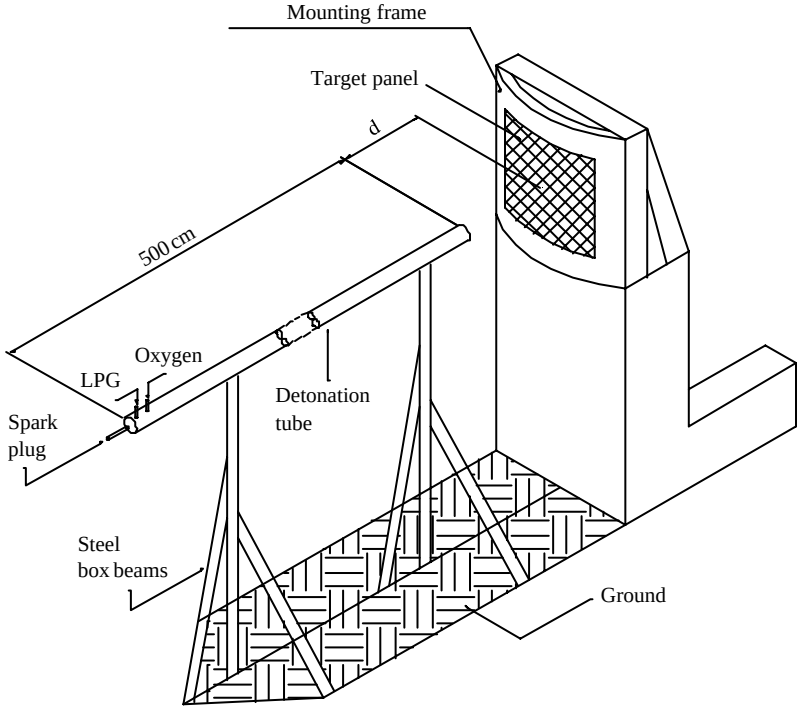

Figure 1. Arrangement of detonation tube, panel mounting frame and panel.

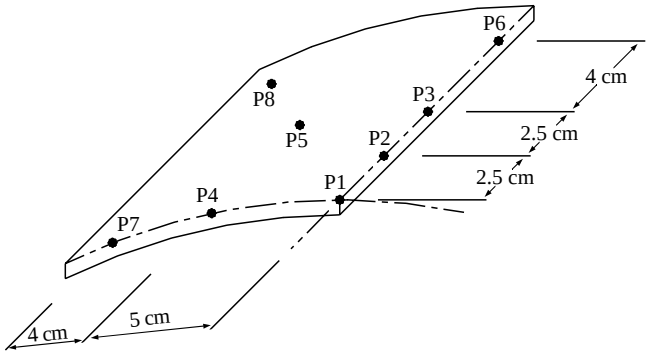

Figure 2. Location of the pressure transducers.

measured by quartz crystal pressure transducers placed on the wooden model which is exposed to the blast loading. The wooden model is mounted 100 cm from the open end of the tube. The detonation tube is centred with respect to the wooden model (Figure 1). Assuming that the distribution of the blast loading on the wooden model is symmetrical, transducers are placed at eight points on a quarter model as shown in Figure 2. The signal obtained from the transducer is amplified using a charge amplifier. The variation of the blast pressure with time is obtained from the blast tests. Blast measurements are repeated three times and average values are calculated.

A strain-gauge and a Wheatstone bridge are used to measure the dynamic strain. The strain gauge is located at the centre and on the back surface of the panel in the longitudinal and circumferential directions. The signal obtained from the bridge circuit is amplified and calibrated by using a dynamic strain-meter. The reader is referred to reference [13] for the detail of the experimental set-up and signal processing.

3. DYNAMIC RESPONSE ANALYSIS

In this section, the mathematical model of the laminated composite panel subjected to blast loading is presented. The resulting time-dependent equation is solved by using Runge–Kutta–Verner method. Furthermore, a finite element model of the problem is developed by the use of ANSYS software. A time-integration technique is then used to solve the blast-loaded panel problem. The laminated composite panel and cylindrical co-ordinate system are depicted in Figure 3.

3.1. GOVERNING EQUATIONS

The displacement field in the shell can be represented by the polynomials or trigonometric series [17]. In the classical shell theory, displacement functions for a cylindrical shell can be written as

$$u = u^0 - z\frac{\partial w^0}{\partial x},$$

$$v = v^0 - z\frac{\partial w^0}{\partial s} + z\frac{v^0}{r},$$

$$w = w^0, \tag{1}$$

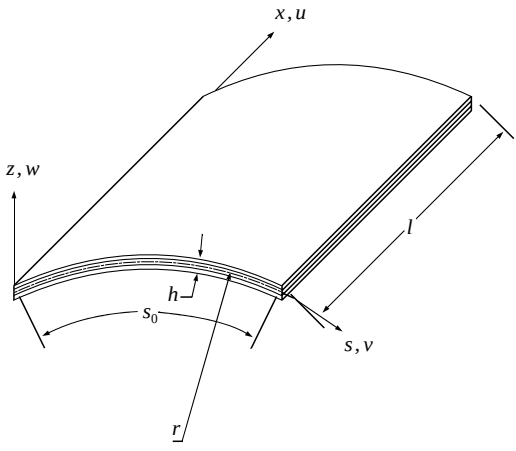

Figure 3. Laminated panel and co-ordinate system.

where u, v and w are the displacement components in the x, s and z directions, u^0, v^0 and w^0 are the displacement components of reference surface in the x, s and z directions, r is the radius of curvature. With this assumption, the strain–displacement relations for the shell can be written as

$$\varepsilon_x = \varepsilon_x^0 + z\kappa_x, \qquad \varepsilon_s = \varepsilon_s^0 + z\kappa_s, \qquad \varepsilon_{xs} = \varepsilon_{xs}^0 + z\kappa_{xs}, \tag{2}$$

where ε_x, ε_s and ε_{xs} are the strains in the shell, ε_x^0, ε_s^0 and ε_{xs}^0 are the membrane strains, κ_x, κ_s and κ_{xs} are the curvatures. Since the panel is subjected to normal blast pressure, the loads in the longitudinal and circumferential directions are assumed to be small in comparison to the load in the normal direction, and in-plane inertia is ignored. In-plane deformations are assumed to be small in comparison to out-of-plane deformations and the loads in the longitudinal and circumferential directions are assumed to be zero. If geometric non-linearities are ignored, the displacements in the shell middle surface, u^0 and v^0, can be assumed to be zero. With this assumption, the membrane strains ε_x^0 and ε_{xs}^0 are zero. The membrane strain in the circumferential direction, ε_s^0, and the curvatures are written as

$$\varepsilon_s^0 = \frac{w^0}{r}, \qquad \kappa_x = -\frac{\partial^2 w^0}{\partial x^2},$$

$$\kappa_s = -\frac{\partial^2 w^0}{\partial s^2}, \qquad \kappa_{xs} = -2\frac{\partial^2 w^0}{\partial s \partial x}. \tag{3}$$

The effective elastic constants are used for defining the mathematical model of the laminated composite. The constitutive equations can then be expressed as [18]

$$\sigma_x = Q_{11}\varepsilon_x + Q_{12}\varepsilon_s + Q_{16}\varepsilon_{xs},$$

$$\sigma_s = Q_{21}\varepsilon_x + Q_{22}\varepsilon_s + Q_{26}\varepsilon_{xs}, \tag{4}$$

$$\sigma_{xs} = Q_{61}\varepsilon_x + Q_{62}\varepsilon_s + Q_{66}\varepsilon_{xs},$$

TABLE 1

Material properties

Properties	Specimen I	Specimen II
E_1 (GPa)	24·14	59·32
E_2 (GPa)	24·14	59·32
G_{12} (GPa)	3·79	3·86
v_{12}	0·11	0·06
ρ (kg/m^3)	1800	1430
r (cm)	25	25

where σ_x, σ_s, and σ_{xs} are stress components, Q_{ij}'s are the elastic constants for a laminated composite and are given by $Q_{11} = E_1/(1 - v_{12}^2)$ $Q_{22} = E_2/(1 - v_{12}^2)$, $Q_{12} = v_{12}E_1/(1 - v_{12}^2)$ $= v_{12}E_2/(1 - v_{12}^2)$, $Q_{16} = Q_{26} = Q_{61} = Q_{62} = 0$ and $Q_{66} = G_{12}$ for the laminated panels used in this study. Here, E_1 and E_2 are moduli of elasticity, G_{12} is shear modulus and v_{12} is the Poisson ratio of the composite material which are given in Table 1. The equation of motion in differential form is written as

$$-\frac{\partial^2 M_x}{\partial x^2} - \frac{\partial^2 M_s}{\partial s^2} - 2\frac{\partial^2 M_{xs}}{\partial x \partial s} + \frac{N_s}{r} - q_z - \bar{m}\ddot{w}^0 = 0, \tag{5}$$

where q_z is the load in the normal direction of the shell, $\dot{w}$ is the velocity, $\ddot{w}$ is the acceleration, $\bar{m}$ is the mass per unit area of the panel which is calculated by multiplying the density (ρ) and the thickness of the panel, N is the stress resultant, and M_x, M_s and M_{xs} are the stress couples. The resultant and couples of the stresses for laminated composite material are given by

$$\begin{aligned} N_s &= A_{22}\varepsilon_s^0 + B_{12}\kappa_x + B_{22}\kappa_s + B_{26}\kappa_{xs}, \\ M_x &= B_{12}\varepsilon_s^0 + D_{11}\kappa_x + D_{12}\kappa_s + D_{16}\kappa_{xs}, \\ M_s &= B_{22}\varepsilon_s^0 + D_{12}\kappa_x + D_{22}\kappa_s + D_{26}\kappa_{xs}, \\ M_{xs} &= B_{26}\varepsilon_s^0 + D_{16}\kappa_x + D_{26}\kappa_s + D_{66}\kappa_{xs}, \end{aligned} \tag{6}$$

where

$$A_{ij} = \sum_{k=1}^{n} (Q_{ij})_k (h_k - h_{k-1}), \qquad B_{ij} = \tfrac{1}{2} \sum_{k=1}^{n} (Q_{ij})_k (h_k^2 - h_{k-1}^2),$$

$$D_{ij} = \tfrac{1}{3} \sum_{k=1}^{n} (Q_{ij})_k (h_k^3 - h_{k-1}^3).$$

Here, h_k denotes the ply thickness. Using the constitutive equations and strain–displacement relations, equation (5) can be written in terms of displacements as

$$L_{33}w^0 + \bar{m}\ddot{w}^0 - q_z = 0, \tag{7}$$

where

$$L_{33} = D_{11}\frac{\partial}{\partial x^4} + 6D_{16}\frac{\partial^4}{\partial x^3 \partial s} + (2D_{12} + 4D_{66})\frac{\partial^4}{\partial x^2 \partial s^2} + 4D_{26}\frac{\partial^4}{\partial x \partial s^3}$$

$$- 2B_{12}/r\frac{\partial^2}{\partial x^2} - 2B_{22}/r\frac{\partial^2}{\partial s^2} - 4B_{26}/r\frac{\partial^2}{\partial x \partial s} + D_{22}\frac{\partial^4}{\partial s^4} + A_{22}/r$$

with the following boundary conditions:

$$w^0(0, s, t) = w^0(\ell, s, t) = w^0(x, 0, t) = w^0(x, s_0, t) = 0,$$

$$\frac{\partial w^0}{\partial x}(0, s, t) = \frac{\partial w^0}{\partial x}(\ell, s, t) = \frac{\partial w^0}{\partial s}(x, 0, t) = \frac{\partial w^0}{\partial s}(x, s_0, t) = 0 \tag{8}$$

and the initial conditions

$$w^0(x, s, 0) = 0, \qquad \dot{w}^0(x, s, 0) = 0. \tag{9}$$

3.2. BLAST LOADING

In this study, the shell is subjected to air blast loading in the direction normal to it and air blast loading is distributed uniformly. The variation of total pressure is given by Friedlander decay function as [4]

$$p(t) = p_m\,(1 - t/t_p)\,\mathrm{e}^{-\alpha t/t_p}, \tag{10}$$

where p is pressure, p_m is peak pressure, t_p is positive phase duration, and α is the waveform parameter.

3.3. SOLUTION OF THE PROBLEM

The translations and rotations are restricted at the clamped boundaries. The displacement function is chosen to satisfy the clamped boundary conditions [15]. The solution is assumed to be the multiplication of co-ordinate and time-dependent parts. With this assumption, the displacement function for clamped shell is given by the following function:

$$w^0 = \sum_{m=1}^{M}\sum_{n=1}^{N} W_{mn}(t)\left(1 - \cos\frac{2m\pi x}{\ell}\right)\left(1 - \cos\frac{2n\pi s}{s_0}\right), \tag{11}$$

where W is time-dependent part of displacement and ℓ and s_0 are the dimensions of the panel in the longitudinal and circumferential directions respectively.

The Galerkin method is used to obtain the system of differential equations of motion which is a function of time. So equation (7) can be written in the following form:

$$\iint_A (L_{33}w^0 + \bar{m}\ddot{w}^0 - q_z)w^0\,\mathrm{d}A = 0. \tag{12}$$

Equation (12) is the linear differential equation of motion of the panel subjected to blast loading. This equation is solved using the Runge–Kutta–Verner method.

3.4. FINITE ELEMENT MODELLING AND ANALYSIS

In addition to the theoretical solution, ANSYS finite element software is used to obtain the strain–time history numerically. The finite element model for the shell consists of an assembly of 3-D shell elements. The shell is discretized by the use of eight-noded laminated shell elements named SHELL91. In the finite element model, no slippage is assumed between the element layers. Shear deflections are included in the element; however, elements normal to the centre plane before deformation are assumed to remain straight after deformation. The stress varies linearly through the thickness of each layer. There are six degrees of freedom at each node [19, 20].

Three different models of Specimen I comprise uniform grids with 36, 64 and 256 shell elements. Comparison of the natural frequencies for the first mode shows a 25% increase when changing the grid mesh from 36 to 64 elements, and a 0·04% decrease when refining this grid from 64 to 256 elements. Convergence of the fundamental frequency shows that the mesh of 64 elements is sufficient to give adequate accuracy.

The pressure load calculated earlier in the previous section is applied on the whole surface of the shell. A total of 200 time function points are used in describing the exponentially decaying blast load. All edges of the shell are modelled by clamped boundary conditions. The linear transient analysis of the shell is performed using the Newmark method based on the time-integration technique.

4. RESULTS AND DISCUSSION

The measured pressure values and their average are shown in Table 2 at 100 cm from the open end of the shock tube. It is observed that the air blast pressure distribution is uniform at 100 cm from the open end of the tube. The pressure–time history obtained from experimental results and an approximate curve fitted by using the Friedlander decay function (equation (10)) is shown in Figure 4. The blast pressure variation measured in the tests shows that the load suddenly increases and then exponentially decays with time. During the decay of blast pressure, some pressure fluctuations are observed.

TABLE 2

Blast test results (*bar*)

Transducer	Test 1	Test 2	Test 3	P_{av}
1	0·293	0·288	0·287	0·289
2	0·287	0·290	0·301	0·293
3	0·267	0·297	0·292	0·285
4	0·296	0·288	0·299	0·294
5	0·298	0·264	0·305	0·289
6	0·297	0·304	0·286	0·296
7	0·299	0·267	0·298	0·288
8	0·295	0·287	0·288	0·290

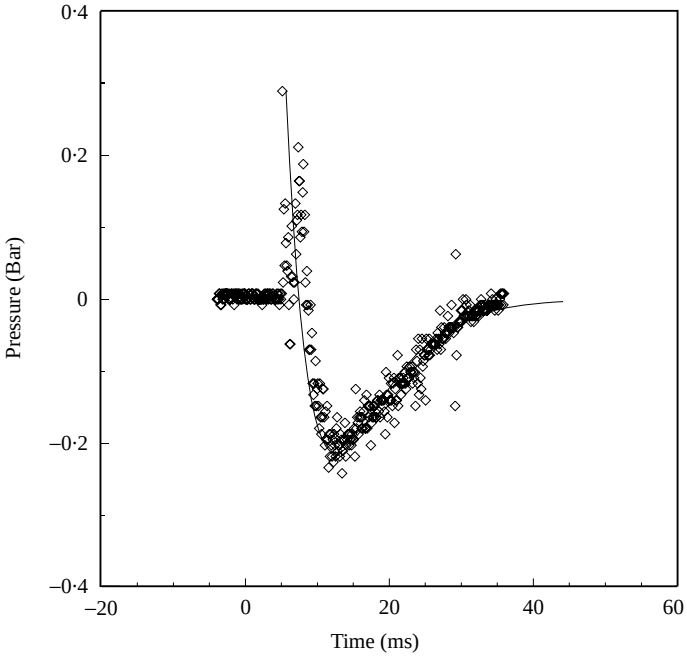

Figure 4. Variation of blast loading with time: ——, approximation; ◇, experimental.

Theoretical, numerical and experimental strain–time histories are obtained for the blast-loaded circular cylindrical laminated panels. The FORTRAN program based on the Runge–Kutta–Verner method is utilized for the theoretical analysis of the laminated composite panels subjected to air blast loading. The time increment is taken to be of the 0·02 ms for all analyses. The theoretical analyses are performed by using one-, four- and nine-term series in the displacement function (equation (11)) for Specimen I. The displacement–time histories of the panel centre are shown in Figure 5. It is assumed that a convergence is obtained with the increasing term numbers because of the agreement between the four- and nine-term series solutions. The dynamic strain–time history of Specimen I in the longitudinal direction is shown in Figure 6. In the longitudinal direction, the positive and negative peak strain levels obtained from theoretical analysis are correlated with the experimental results. The peak strain levels are over-predicted by ANSYS. The dynamic strain–time history of Specimen I in the circumferential direction is shown in Figure 7. The strain–time history curves obtained from theoretical and numerical analyses are well correlated with the experimental results until 0·7 ms. A discrepancy occurred between the predicted and measured strains after 0·7 ms. The load in the circumferential direction is taken as zero in the theoretical solution. However, the ignored load in the circumferential direction is larger than the ignored load in the longitudinal direction. Therefore, a discrepancy occurs between the theoretical and experimental results. The compatibility of chosen displacement functions with the curved surface can be one reason for the discrepancy shown between the experimental and theoretical circumferential strains. The chosen displacement functions show better compatibility with the flat surface. The positive and negative peak strain levels are over-predicted by ANSYS beyond 0·7 ms. The blast pressure is applied to the whole surface at the same time in the analysis, but the blast pressure arrives first at the centre of the panel in the test. This situation can also be a reason for the discrepancy between the theoretical, numerical and experimental results. The

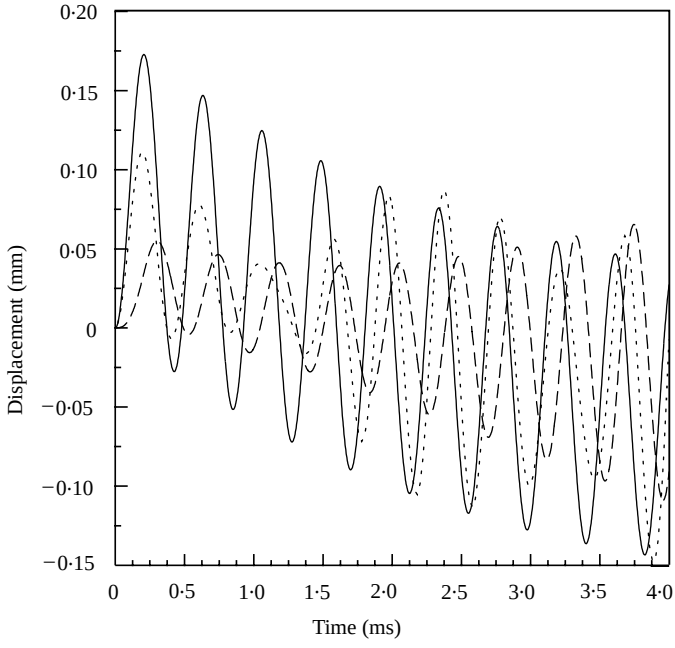

Figure 5. Effect of the term number on the analysis: ——, 1 term; – – –, 4 terms; ·····, 9 terms.

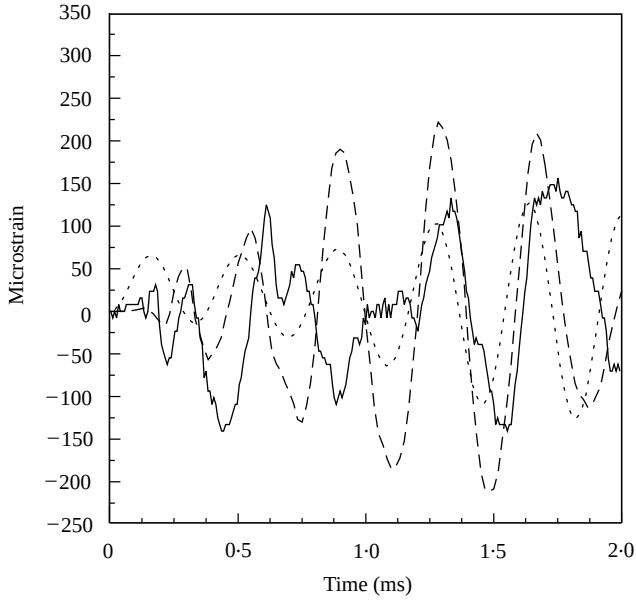

Figure 6. Comparison of the strain–time history results in the longitudinal direction for Specimen I: ——, experiment; ·····, theoretical (9 terms); – – – –, ANSYS.

dynamic strain–time histories of Specimen II in the longitudinal and circumferential directions are shown in Figures 8 and 9 respectively. The peak strain levels are under-predicted in the theoretical analysis in the longitudinal and circumferential directions. Specimen II has smaller density than Specimen I. Meanwhile the out-of-plane

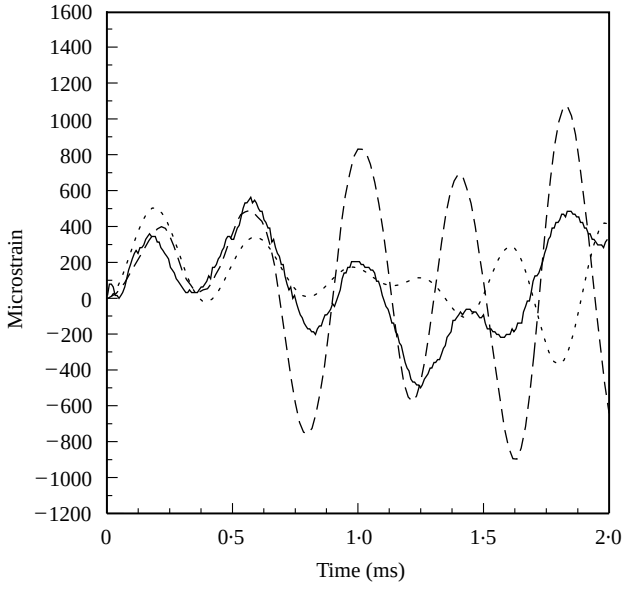

Figure 7. Comparison of the strain–time history results in the circumferential direction for Specimen I: ——, experiment; ·····, theory (9 terms); – – – –, ANSYS.

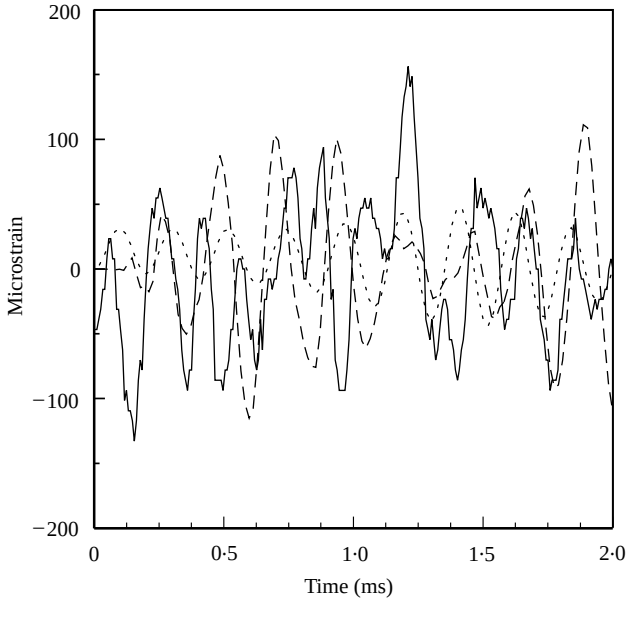

Figure 8. Comparison of the strain–time history results in the longitudinal direction for Specimen II: ——, experiment; ·····, theory (9 terms); – – – –, ANSYS.

inertia of Specimen II is smaller than that of Specimen I. Therefore, ignoring the in-plane inertia of Specimen II increases the peak strain level differences between the theoretical and experimental results. The positive and negative peak strain levels of Specimen II are over-predicted by ANSYS.

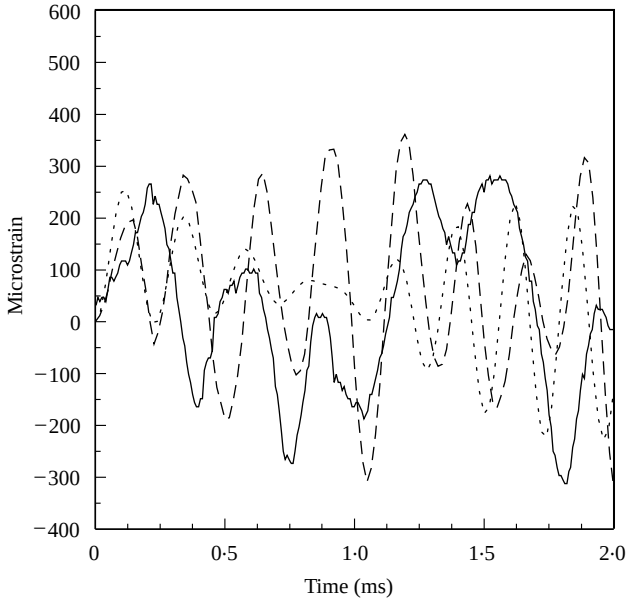

Figure 9. Comparison of the strain–time history results in the circumferential direction for Specimen II: ——, experiment; ·····, theory (9 terms); – – – –, ANSYS.

It is observed that the peak strain levels of Specimen I, especially in the circumferential direction, are bigger than those of Specimen II. It is also observed that the response frequencies of Specimen I in the longitudinal and circumferential directions are smaller than those of Specimen II. These two observations can be explained by the material and geometrical properties. The moduli of elasticity of Specimen II are bigger than those of Specimen I, and the density and thickness of Specimen II are smaller than those of Specimen I. The larger moduli of elasticity and the smaller mass cause smaller peak strain levels and the higher response frequency. This situation can also be seen in equation (12). It is found that Specimen II has better dynamic characteristics in comparison with Specimen I, when they are subjected to blast load.

The power spectral density, a measurement of the energy at various frequencies, is calculated to identify the frequency components. The fast Fourier transformation technique is used for the spectral analysis of the strain–time history results of Specimen I. The power spectra of the longitudinal strain–time data obtained from the experimental, theoretical and numerical results are shown in Figure 10. The dominant frequencies of longitudinal strains obtained from the experimental, theoretical and numerical results are 2800, 3000 and 2520 Hz respectively. A secondary response frequency of 500 Hz is shown in Figure 10 for the experimental and theoretical results. The longitudinal strain–time response frequency is predicted well using the theoretical method. The frequency of longitudinal strain obtained from the numerical results shows a little difference from the theoretical prediction because the calculated stiffness in the numerical analysis is smaller than the calculated stiffness in the theoretical analysis. This situation is consistent with the over-prediction of the peak strain levels in the numerical analysis. The power spectra of the circumferential strain–time data obtained from the experimental, theoretical and numerical results are shown in Figure 11. The dominant frequencies of circumferential strains obtained from the experimental, theoretical and numerical results are 250, 2500 and 2694 Hz respectively. The theoretical and numerical results of the response frequency show a large difference from the

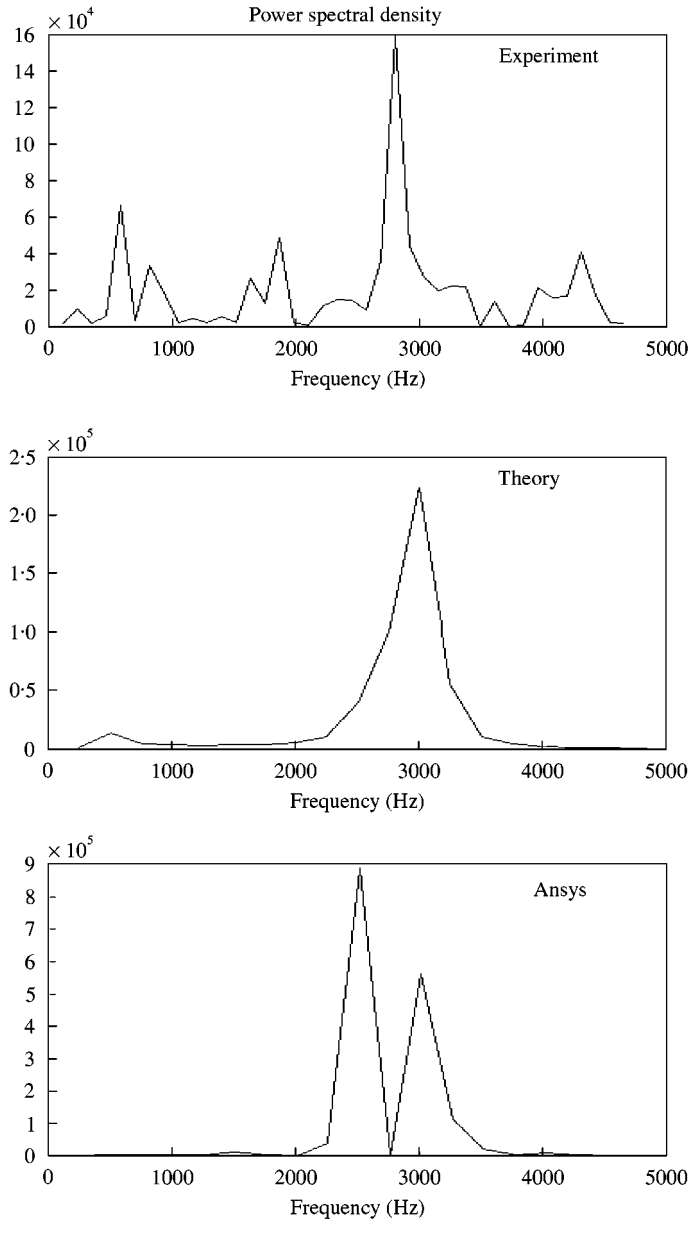

Figure 10. The spectral analysis results in the longitudinal direction.

experimental results in the circumferential direction. The secondary response frequencies of circumferential strains obtained from the experimental, theoretical and numerical analyses are 2700, 500 and 1500 Hz respectively. The first two dominant frequencies of the circumferential strains obtained from the experimental and theoretical results are in an agreement but in a different order. In other words, the experimental results show that the primary and secondary frequencies of the circumferential strain are 250 and 2700 Hz, respectively, while the theoretical prediction of the primary and secondary response frequencies of the circumferential strain are 2500 and 500 Hz respectively.

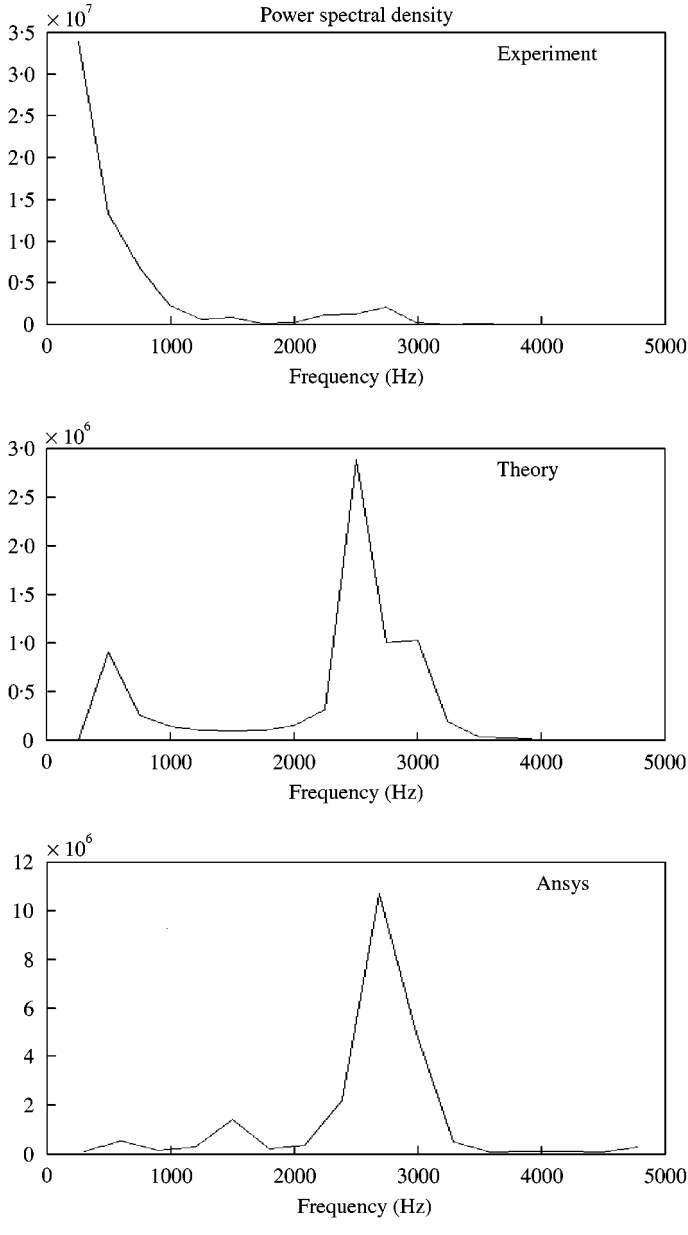

Figure 11. The spectral analysis results in the circumferential direction.

5. CONCLUSIONS

This paper presents a theoretical analysis and correlation with the experimental results of the strain–time histories of laminated composite cylindrical panels exposed to normal blast shock waves. The blast wave is assumed that decaying exponentially with time and uniformly distributed on the panel surface. The equation of motion of the panel is solved using the Runge–Kutta–Verner method and the theoretical results are compared with the experimental and finite element results for the laminated cylindrical composite panels. The

following conclusions apply to laminated cylindrical composite panels with clamped boundary conditions as considered herein.

An agreeable approximation to the blast test result is achieved by using the Friedlander decay function. However, some pressure fluctuations are observed in the blast pressure time variation obtained from experimental results. The pressure fluctuations are not included in the analyses.

The peak strain levels and response frequencies of Specimen I in the longitudinal direction obtained by using theoretical analysis and experimental results are in a good agreement. However, a considerable difference is shown between the strain–time histories in the circumferential direction obtained from theoretical and experimental methods after 0·7 ms. The response frequency, which has great importance in dynamic phenomena, is predicted by using the theoretical method successively in the longitudinal direction. Thus, the theoretical solution may be used to provide material for a preliminary design. On the other hand, the chosen displacement functions show better compatibility with the flat surface than curved surface. The peak strain levels of Specimen II are under-predicted by theoretical analysis. The peak strain levels of Specimens I and II are over-predicted in the longitudinal and circumferential directions using ANSYS. The response frequency obtained from the numerical method is smaller than the response frequency obtained from the theoretical method. These two results are due to the smaller calculated stiffness in the finite element analysis.

The effect of structural damping is not taken into account in this study. However, the effect of structural damping and loading conditions on the dynamic response of the laminated composite panel can be examined by this method. The cut-out effects can be investigated for composite panel structures. The hygro-thermal effects may be interesting in respect of the dynamic response of panel. The measurement of the panel displacements and examination of the displacement functions for the curved surface will be investigated in future studies.

REFERENCES

1. L. A. Pilato and M. J. Michna 1994 *Advanced Composite Materials*. New York: Springer-Verlag, 157–185.
2. R. Houlston, J. E. Slater, N. Pegg and C. G. Desrochers 1985 *Computers and Structures* **21**, 273–289. On analysis of structural response of ship panels subjected to air blast loading.
3. R. Houlston and C. G. Desrochers 1987 *Computers and Structures* **26**, 1–15. Nonlinear structural response of ship panels subjected to air blast loading.
4. A. D. Gupta, F. H. Gregory, R. L. Bitting and S. Bhattacharya 1987 *Computers and Structures* **26**, 339–344. Dynamic analysis of an explosively loaded hinged rectangular plate.
5. G. N. Nurick, M. D. Olson, J. R. Fagnan and A. Levin 1995 *International Journal of Impact Engineering* **16**, 273–291. Deformation and tearing of blast-loaded stiffened square plates.
6. D. Redekop and P. Azar 1991 *Journal of Vibration and Acoustics* **113**, 273–278. Dynamic response of a cylindrical shell panel to explosive loading.
7. D. Redekop 1994 *Computers and Structures* **51**, 126–133. Dynamic response of a toroidal shell panel.
8. J. Jiang and M. D. Olson 1991 *Computers and Structures* **41**, 41–52. Nonlinear dynamic analysis of blast loaded cylindrical shell structures.
9. M. D. Olson 1991 *Computers and Structures* **40**, 1139–1149. Efficient modelling of blast loaded stiffened plate and cylindrical shell structures.
10. J. N. Reddy 1983 *American Institute of Aeronautics and Astronautics Journal* **21**, 621–629. Geometrically nonlinear transient analysis of laminated composite panels.
11. L. Librescu and A. Nosier 1990 *American Institute of Aeronautics and Astronautics Journal* **28**, 345–352. Response of laminated composite flat panels to sonic boom and explosive blast loadings.

12. H. S. TÜRKMEN 1998 *Ph.D. Thesis*, *Istanbul Technical University*, 72 + xviii. Dynamic response of laminated composite panels subjected to blast loading.
13. H. S. TÜRKMEN and Z. MECİTOĞLU 1999 *Journal of Sound and Vibration* **221**, 371–389. Dynamic response of a stiffened laminated composite plate subjected to blast load.
14. H. S. TÜRKMEN and Z. MECİTOĞLU 1999 *American Institute of Aeronautics and Astronautics Journal* **37**, 1639–1647. Nonlinear structural response of laminated composite plates subjected to blast loading.
15. H. S. TÜRKMEN 1999 *ARI* **51**, 175–180. Structural response of cylindrically curved laminated composite shells subjected to blast loading.
16. H. S. TÜRKMEN and Z. MECİTOĞLU 1998 35*th Annual Technical Meeting of the Society of Engineering Science*. Washington State University, Pullman, Washington, U.S.A. Structural response of laminated composite shells subjected to blast loadings.
17. Z. MECİTOĞLU 1996 *American Institute of Aeronautics and Astronautics Journal* **34**, 2118–2125. Governing equations of a stiffened laminated inhomogeneous conical shell.
18. K. K. CHAWLA 1987 *Composite Materials*. New York: Springer-Verlag, 204–258.
19. ANSYS5.3 Elements Reference, 000655, 1996 SAS IP, Inc., ANSYS Headquarters, Canonsburg PA, U.S.A. Chapter 4, eighth edition, pp. 625–636, October.
20. ANSYS5.3 Elements Reference, 000656, 1996 SAS IP, Inc., ANSYS Headquarters, Canonsburg PA, U.S.A. Chapter 14, seventh edition, pp. 344–350, June.